Improving resolution by the higher-order microscope imaging system with thermal light

Yanfeng Bai*
Department of Physics, Southeast University, Nanjing 210096, China
(Dated: February 27, 2014)

The resolution properties of the higher-order ghost imaging with thermal light source are investigated. In a multi-arm microscope imaging scheme with thermal light, we compare the resolution of the images obtained by the higher-order correlation with that by the lower-order correlation, and show that the resolution of the images can be enhanced with an increasing number of the reference arms. The effects from the aperture of the reference lens are also discussed.

PACS numbers:

I. INTRODUCTION

In recent years, ghost imaging, ghost interference, and subwavelength interference have been investigated extensively both in quantum field and classical field. The first coincidence imaging experiment was performed based on entangled photon pairs generated by spontaneous parametric down-conversion (SPDC)[1]. While Bennink *et al.* provided an experimental demonstration of ghost imaging by using a classical source[2]. Compared with entangled source, the visibility of the second-order correlated imaging with thermal source is quite low, which could become the obstacle for the applications of the imaging technique. To enhance the visibility, some efforts turned to higher-order ghost imaging[3–7]. As pointed in Refs. [4, 5], the higher-order intensity correlation could improve the visibility and the resolution of the interference pattern in a double-slit interference scheme when compared with the lower-order intensity correlation. However, their work focused on the higher-order ghost interference and diffraction, the resolution of the higher-order ghost imaging was not mentioned. In this Letter, we discuss the higher-order microscope imaging with thermal source. Based on the analytical results and the numerical simulations, we show that the resolution of the images can be enhanced with an increase of the reference arms in a multi-arm microscope imaging system.

II. THE MODEL AND ANALYTICAL RESULTS

Here, the test arm is a conventional imaging setup, and the object distance z_1, the image distance z_{12}, and the focal length of the objective lens f_1 obey the Gaussian thin-lens equation: $1/z_1 + 1/z_{12} = 1/f_1$. Based on the Rayleigh criterion, the resolution limit δx of the test arm is determined by the wavelength and the NA of the objective lens: $\delta x = 0.61\lambda/\mathrm{NA} \simeq \lambda z_1/a_1$, where a_1 is the aperture of the objective lens. For simplicity, we suppose that

*Corresponding author. E-mail: yanfengbai@gmail.com.

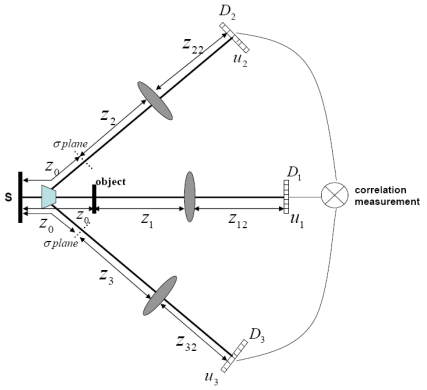

FIG. 1: A three-arm microscope imaging system.

the distance z_i, z_{i2} and f_i also satisfy the Gaussian thin-lens equation in the reference arm: $1/z_i + 1/z_{i2} = 1/f_i$. Under the paraxial approximation, the impulse response functions for the i arms can be derived from the Huygens-Fresnel integral[9], we do not show them here.

Based on the previous work[5], the information of the object can be retrieved by measuring the i-order intensity correlation between the i detectors. For simplicity and without losing generality, we firstly give the results under the third-order correlation[3], then generalize the higher-order case.

$$G^{(3)}(u_1,u_2,u_3) = \langle I_1\rangle\langle I_2\rangle\langle I_3\rangle + \langle I_1\rangle G_{23} + \langle I_2\rangle G_{13} + \langle I_3\rangle G_{12} + G_{123}, \quad (1)$$

where the first two terms on the right-hand side of Eq. (1) contribute only the background, the third and the fourth terms involve two-photon bunching[5], and give the information of the object imaged at D_2 and D_3, respectively. This is the phenomenon of the second-order ghost imaging in essence. The last term which involves three-photon bunching represents the intensity fluctuation correlation between three detectors, we only discuss the contribution from this term in the following. During of this process, a double-slit with the slit width $b = 0.04$mm and the distance between two slits $d = 0.08$mm is chosen as the object imaged, and it is placed at $z_0 = 100$mm from the

978-1-4673-5225-3/14/$31.00 ©2014 IEEE

light source. $z_i = 150$mm and $z_{i2} = 300$mm are chosen to obtain the same magnification $M_i = 2$, and we assume that objective and the reference lenses have the same focal length $f_i = 100$mm. The aperture of the objective lens is fixed $a_1 = 2$mm, and the aperture of the reference lens is variable.

By substituting the corresponding impulse response functions into Eq. (1), and assuming the source is large enough and the intensity distribution is uniform $I(x) = I_0$, we can get the expression of the intensity fluctuation correlation between three detectors. Here we assume that two reference detectors are scanned synchronously, i.e., $u_2 = u_3$, for a simple case of $u_1 = u_i M_1/M_i$, we have

$$\begin{aligned} G_{123}(u_i\frac{M_1}{M_i}, u_i) &= \Big| \int d\nu_1 t(\nu_1) \mathrm{sinc}\Big[\frac{a_1}{\lambda d_1}\Big(\nu_1 + \frac{u_i}{M_i}\Big)\Big] \\ &\quad \times \mathrm{sinc}\Big[\frac{a_i}{\lambda d_i}\Big(\nu_1 + \frac{u_i}{M_i}\Big)\Big]\Big|^2 \\ &\quad \times \int d\nu_i \mathrm{sinc}^2\Big[\frac{a_i}{\lambda d_i}\Big(\nu_i + \frac{u_i}{M_i}\Big)\Big], \quad (2) \end{aligned}$$

where some unessential constant (phase) factors have been omitted. The corresponding image represents the point-point intensity correlation function, and its integral kernel

$$\begin{aligned} & H_3(u_i\frac{M_1}{M_i}, u_i) \\ &= \mathrm{sinc}\Big[\frac{a_1}{\lambda d_1}\Big(\nu_1 + \frac{u_i}{M_i}\Big)\Big]\mathrm{sinc}\Big[\frac{a_2}{\lambda d_2}\Big(\nu_1 + \frac{u_i}{M_i}\Big)\Big] \\ &\quad \times \mathrm{sinc}\Big[\frac{a_3}{\lambda d_3}\Big(\nu_1 + \frac{u_i}{M_i}\Big)\Big], \quad (3) \end{aligned}$$

it is not difficult to give the corresponding expression under the i-order intensity correlation measurement.

$$\begin{aligned} & H_i(u_i\frac{M_1}{M_i}, u_i) \\ &= \mathrm{sinc}\Big[\frac{a_1}{\lambda d_1}\Big(\nu_1 + \frac{u_i}{M_i}\Big)\Big]\mathrm{sinc}\Big[\frac{a_2}{\lambda d_2}\Big(\nu_1 + \frac{u_i}{M_i}\Big)\Big] \\ &\quad \times \cdots \times \mathrm{sinc}\Big[\frac{a_i}{\lambda d_i}\Big(\nu_1 + \frac{u_i}{M_i}\Big)\Big]. \quad (4) \end{aligned}$$

The point spread function $H_i(u_i M_1/M_i, u_i)$ characterizes the resolution of the higher-order ghost imaging system. Obviously, the resolution depends the number of the reference arms and the apertures of the reference lenses a_i if the NA of the objective lens is limited. Both using large apertures and increasing the number of the reference arms can result in the improvement of the resolution.

In the following, we show the numerical simulations to demonstrate the above results. In the above calculation and discussion, we have assumed that the source is large enough and the intensity distribution is uniform. In the practical case, this source does not exist. Here we assume that intensity distribution of the source is of the Gaussian type. Figure 2 gives the resolution difference between the images obtained by the third-order correlated imaging and by the lower-order one. When we only consider the test arm, the resolution limit of the test arm $\delta x \simeq 1.22\lambda z_1/a_1 \approx 0.05$mm is smaller than the two-slit separation 0.08mm. Thus we can not obtain the images of the two-slit only by the imaging setup of the test arm, as shown in Fig. 2(a). Then, a conventional lens-limited imaging system is rebuilt into a two-arm endoscope by adding a reference arm, the result is plotted in Fig. 2(b). Here we can distinguish the two slits which are obtained by the intensity correlation between D_1 and D_2, while the resolution of the images is not good, and definitely needs to be improved.

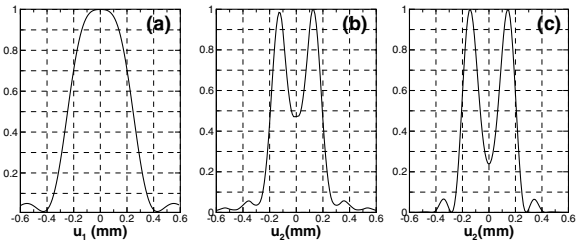

FIG. 2: The images of the two-slit from (a) only the test arm, (b) the second-order intensity correlation between the test arm and one reference arm, and (c) the third-order intensity fluctuation correlation between three detectors. Other parameters are chosen as $\lambda = 532$nm, $a_2 = a_3 = 1$mm, and the transverse size of the source $\sigma_I = 0.5$mm.

Now, the most obvious question is whether the imaging resolution can be improved by considering higher-order correlated imaging. To this end, we need compare the results from third-order intensity correlation with that in Fig. 2(b). While it is quite difficult to compare a two-dimensional image with a three-dimensional one. Based on the conclusion in Ref. [5], we know that the contribution from three-photon bunching to the final imaging is equal to the sum of the two-photon bunching effects only when the condition of $u_2 = u_3$. So we use the sum of the two-photon bunching effects for $u_2 = u_3$ to replace the imaging signal from three-photon bunching, the result is shown in Fig. 2(c). It is shown that by comparing Figs. 2(b) and (c), the resolution is enhanced greatly when two additional reference arms are considered.

We next explore the effects from another parameter in Eq. (3), i.e., the apertures of the reference lenses. With the apertures of the reference lenses increasing from $a_i = 1$mm in Fig. 2 to $a_i = 5$mm in Fig. 3, the two slits are separated clearly. In other words, an increasing aperture of the reference lens makes the resolution of the images improve evidently.

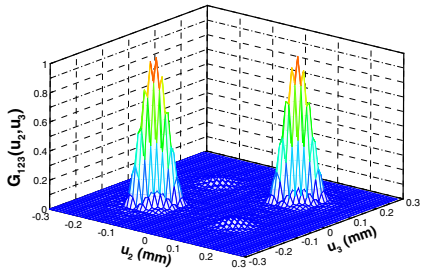

FIG. 3: The same as Fig. 2 except for $a_2 = a_3 = 5$mm.

III. CONCLUSIONS

In conclusion, we have investigated the higher-order microscope imaging with thermal light. Based on the theoretical analysis and the numerical simulations, we show that both large apertures of the reference lenses and an increasing number of the reference arms enhance the imaging resolution. Our results can be applied to improve the resolution of a conventional lens-limited imaging system. For example, the medical video endoscope can be substituted with a multi-arm endoscope by adding the number of the reference arms. Here we can use large reference lenses to enhance the resolution. If the reference arms have limitation in size, higher-resolution images can be also obtained by considering more reference arms.

Acknowledgments

This work is partially supported by the National Natural Science Foundation of China (Grant No. 61372102).

[1] T. B. Pittman, Y. H. Shih, D. V. Strekalov, and A. V. Sergienko, "Optical imaging by means of two-photon quantum entanglemnt," *Phys. Rev. A*, **52,** 1995, pp. R3429-R3432.

[2] R. S. Bennink, S. J. Bentley, and R. W. Boyd, "Two-photon coincidence imaging with a classical source," *Phys. Rev. Lett.*, **89,** 2002, pp. 113601-1-4.

[3] Y. F. Bai and S. S. Han, "Ghost imaging with thermal light by third-order correlation," *Phys. Rev. A*, **76,** 2007, pp. 043828-1-4.

[4] D. Z. Cao, J. Xiong, S. H. Zhang, L. F. Lin, L. Gao, and K. G. Wang, "Enhancing visibility and resolution in Nth-order intensity correlation of thermal light," *Appl. Phys. Lett.*, **92,** 2008, pp. 201102-1-3.

[5] Q. Liu, X. H. Chen, K. H. Luo, W. Wu, and L. A. Wu, "Role of multiphoton bunching in high-order ghost imaging with thermal light sources," *Phys. Rev. A*, **79,** 2009, pp. 053844-1-8.

[6] Y. Zhou, J. Simon, J. B. Liu, and Y. H. Shih, "Third-order correlation function and ghost imaging of chaotic thermal light in the photon counting regime," *Phys. Rev. A*, **81,** 2010, pp. 043831-1-9.

[7] B. Cao and C. Zhang, "Third-order lensless ghost diffraction with classical fully incoherent light," *Opt. Lett.*, **35,** 2010, pp. 2091-2093.

[8] P. L. Zhang, W. L. Gong, X. Shen, D. J. Huang, and S. S. Han, "Improving resolution by the second-order correlation of light fields," *Opt. Lett.*, **34,** 2009, pp. 1222-1224.

[9] J. W. Goodman, Introduction to Fourier Optics (McGraw-Hill, 1968).